JPE 19-6-18

https://doi.org/10.6113/JPE.2019.19.6.1527
ISSN(Print): 1598-2092 / ISSN(Online): 2093-4718

Passivity-Based Control System of Permanent Magnet Synchronous Motors Based on Quasi-Z Source Matrix Converter

Qiming Cheng* and Lin Wei†

†,*College of Automation Engineering, Shanghai University of Electric Power, Shanghai, China

Abstract

Because of the shortcomings of the PID controllers and traditional drive systems of permanent magnet synchronous motors (PMSMs), a PMSM passivity-based control (PBC) drive system based on a quasi-Z source matrix converter (QZMC) is proposed in this paper. The traditional matrix converter is a buck converter with a maximum voltage transmission ratio of only 0.866, which limits the performance of the driven motor. Therefore, in this paper a quasi-Z source circuit is added to the input side of the two-stage matrix converter (TSMC) and its working principle has also been verified. In addition, the controller of the speed loop and current loop in the conventional vector control of a PMSM is a PID controller. The PID controller has the problem since its parameters are difficult to adjust and its anti-interference capability is limited. As a result, a port controlled dissipative Hamiltonian model (PCHD) of a PMSM is established. Thereafter a passivity-based controller based on the interconnection and damping assignment (IDA) of a QZMC-PMSM is designed, and the stability of the equilibrium point is theoretically verified. Simulation and experimental results show that the designed PBC control system of a PMSM based on a QZMC can make the PMSM run stably at the rated speed. In addition, the system has strong robustness, as well as good dynamic and static performances.

Key words: Passivity-based control, Permanent magnet synchronous motor, Quasi-Z source, Two-stage matrix converter

I. INTRODUCTION

Permanent Magnet Synchronous Motors (PMSMs) have the virtues of a simple structure, stable operation, small size and high efficiency. With the continuous improvement of materials and control technologies, PMSMs have been widely used in civil manufacturing, aerospace and military fields [1]. The conventional power electronic driving devices of a PMSM, such as DC-AC inverters and AC-DC-AC converters, have disadvantages such as low voltage transmission ratio, large intermediate DC capacitors, and the fact that they cannot be integrated [2].

As a kind of AC-AC inverter, the quasi-Z source indirect matrix converter is composed of a quasi-Z source circuit and a two-stage matrix converter (TSMC). There is no DC capacitor between the rectifier stage and the inverter stage of the two-stage matrix converter, which overcomes the shortcomings of the traditional AC-DC-AC converters, where DC capacitor cannot be integrated [3]. However, its maximum voltage transmission ratio is 0.866 [4]. According to the authors of [5], when the motor is driven, the three-phase stator voltage is lower than the rated voltage. As a result, the motor cannot work at the rated speed, which limits the speed regulation range of the PMSM. In addition, the low voltage is unfavorable for the PMSM startup, which can damage the motor when driving a heavy load [5].

In [6], the over-modulation method is used to improve the voltage transfer ratio of a TSMC. However, the low order harmonics of the output voltage and input current are introduced, and an LC filter needs to be added to the input side of the TSMC, which increases the cost. The quasi-Z source circuit can effectively improve the voltage utilization by inserting a through-vector, and there is no need to insert a dead zone commutation time. The authors of [7] analyzed various Z-source matrix converter topologies and noted that when an input current continuous type quasi-Z is added, an LC filter on the input side does not need to be added. The

---

Manuscript received Apr. 23, 2019; accepted Jul. 12, 2019
Recommended for publication by Associate Editor Honnyong Cha.

†Corresponding Author: 1423703459@qq.com
Tel: +86 18621558524, Shanghai University of Electric Power
*College of Autom. Eng., Shanghai University of Electric Power, China

authors of [8] modeled a Z-source matrix converter and verified its stability. Therefore, the quasi-Z source matrix converter (QZMC) combined with the quasi-Z source network and the TSMC has significant advantages, which has attracted a lot of attention from scholars in the motor drive field [9], [10]. PMSM control systems mostly use basic vector control and direct torque control methods [11]. Among them, the vector control can decouple the AC and DC components of the stator current, and realize the decoupling control of the magnetic field and the torque. Therefore, it has been widely used in the motor control. This method generally uses a PID regulator as the controller. However, a PMSM is a nonlinear, strongly coupled system, which is great impacted by the control effect when it is disturbed by external disturbances or motor parameters. In [12], model reference adaptive control is used to solve the problem of model robustness. However, establishing the model and the time constraint of online correction limit its application range. In [13], sliding mode control (SMC) is applied to a PMSM speed control system. In order to suppress the chattering phenomenon of SMC, the sliding mode approach law is improved in [14]. However, the time to get close to the sliding mode surface is longer. In [15], backstepping control is applied to PMSM control. The controller has global stability. However, there are some problems with this approach since the speed control has a static error and the overshoot is large. Therefore, some scholars have done research on the combination of adaptive and backstepping control [16], [17]. However, the time constraint problem of adaptive control has not been solved.

Passivity-based control (PBC) is a non-linear feedback energy control method that uses the reactive component assignment on the system dissipative characteristic equation to ensure that the system energy follows a given energy function. Therefore, the system state variable can reach a given value. PBC has the advantages of a fast dynamic response, strong anti-interference capability, simple structure and easy implementation, and it has already been applied in PWM rectifier control [18]-[21].

This study proposes a PBC drive system for a PMSM based on a QZMC. This paper is organized as follows. Section II describes the overall structure of the designed system. Section III introduces the model and principle of a QZMC. The PBC controller is analyzed and designed in Section IV and Section V. Simulation and experimental results are presented in Section VI and Section VII to validate the proposed system. Finally, some conclusions are presented in Section VIII.

II. OVERALL STRUCTURE OF A QZMC-PMSM PBC CONTROL SYSTEM

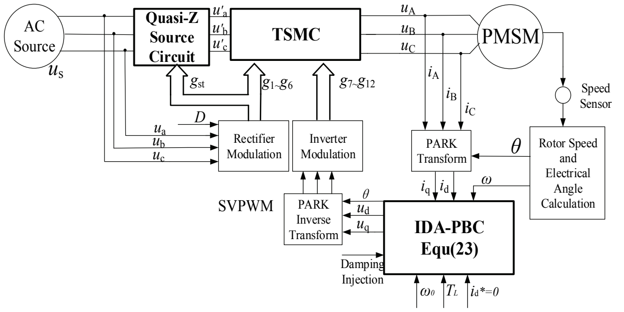

Fig. 1. Structure diagram of a passivity-based control system for the QZMC-PMSM.

Fig. 1 presents a structure diagram of the proposed passivity-based control system for the QZMC-PMSM. In this system, the rectifier stage modulation of the QZMC adopts the SVPWM modulation method [22], which inserts the through-vector, and obtains 7 PWM pulses g_{st} and g_1~g_6 from the AC power supply phase voltages u_a, u_b, u_c and the through-duty D. Among them, g_{st} is a through pulse, which is used to control the through and non-through state switchings of the quasi-Z source network. As a result, the quasi-Z source network outputs the boosted voltages u'_a, u'_b, u'_c; and g_1~g_6 are used to control the rectifier stage switching action.

The PID controller used in traditional vector control has the disadvantages of difficult parameter adjustment, poor dynamic performance and poor robustness. Therefore, the PMSM controller in this paper uses a nonlinear PBC controller based on interconnection and damping assignment (IDA) [23]. The output obtained by the passivity-based controller is supplied to the inverter stage modulation module to control the PMSM. The PMSM passivity-based controller outputs the dq axis stator voltages u_d and u_q. The three-phase stator voltages u_A, u_B and u_C are obtained from the anti-PARK abc coordinates. The inverter stage modulates u_A, u_B and u_C by the SVPWM modulation algorithm, and outputs six PWM pulses g_7~g_{12} are used to control the inverter stage switching action.

III. WORKING PRINCIPLE AND MODELING OF A QZMC

A. Topology of the Quasi-Z Source Matrix Converter

The quasi-Z source matrix converter topology is shown in Fig. 2. This topology consists of three identical current-continuous quasi-Z source networks and a two-stage matrix converter. The traditional matrix converter has a maximum voltage gain of only 0.866, which limits the speed range of the driven motor. The boosting characteristic of the quasi-Z source circuit increases the speed range of the motor. This section demonstrates the principle of the quasi-Z source circuit.

B. Boost Principle of the Quasi-Z source Circuit

When the Z source circuit is analyzed, the inverter stage of the two-stage matrix converter can be equivalent to a two-port

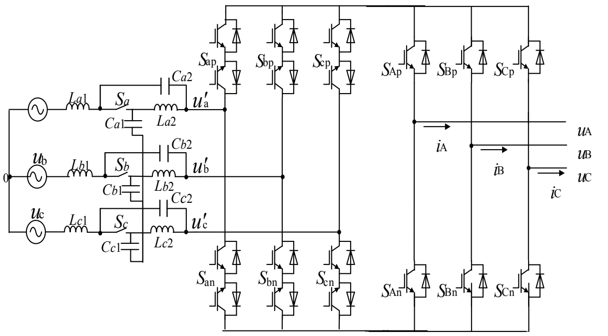

Fig. 2. Topology of the quasi-Z source matrix converter.

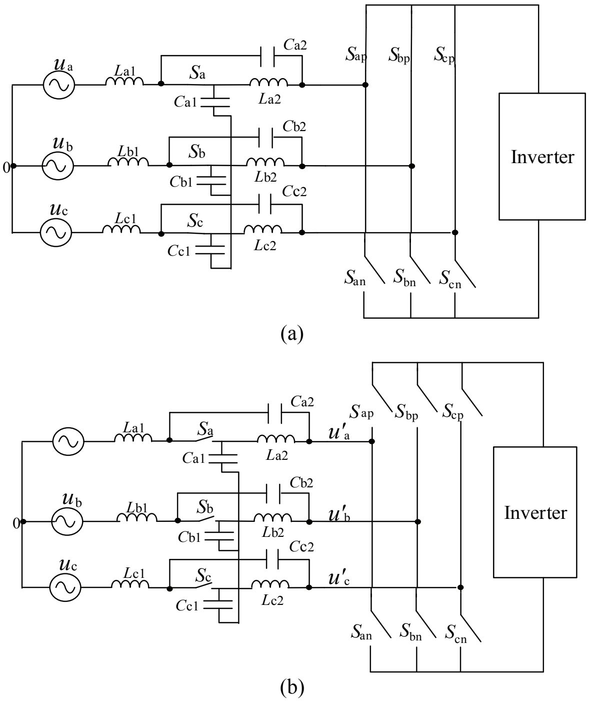

(a)

(b)

Fig. 3. Equivalent circuit of a quasi-Z source matrix converter. (a) Non-through state equivalent circuit. (b) Through state equivalent circuit.

network. According to the symmetrical structure of the three-phase quasi-Z source network:

$$\begin{cases} L_{a1}=L_{a2}=L_{b1}=L_{b2}=L_{c1}=L_{c2}=L \\ C_{a1}=C_{a2}=C_{b1}=C_{b2}=C_{c1}=C_{c2}=C \end{cases} \tag{1}$$

Fig. 3 is an equivalent circuit of a quasi-Z source matrix converter. When the QZMC is operating in the non-through state, the switch S_x is turned on, and the equivalent circuit is shown in Fig. 3(a). The quasi-Z source network is three-phase symmetrical, and phase a is taken as an example to derive the boosting principle. The circuit is now satisfied:

$$\begin{cases} u_{L_{a2}}=-u_{C_{a2}} \\ u_{L_{a1}}=u_a-u_{C_{a1}} \\ u_{L_{a1}}=u_a+u_{Ca2}-u'_a \end{cases} \tag{2}$$

Where $u_{L_{a1}}$, $u_{L_{a2}}$ and $u_{C_{a1}}$, $u_{C_{a2}}$ are the voltages across the inductors L_{a1} and L_{a2} and the capacitors C_{a1} and C_{a2}, respectively.

When the quasi-Z source matrix converter operates in the through state, the switch S_x is turned off, and the equivalent circuit is shown in Fig. 3(b). The circuit is now satisfied:

$$\begin{cases} u_{L_{a2}}=u_{C_{a1}} \\ u_{L_{a1}}=u_a+u_{C_{a1}} \end{cases} \tag{3}$$

According to the volt-second principle, the average value of the voltage across the inductor in one cycle during a switching cycle T_s should be zero, which is obtained by Eqns. (2)-(3):

$$\begin{cases} (1-D)\left(-u_{C_{a2}}\right)+Du_{C_{a1}}=0 \\ (1-D)\left(u_a-u_{C_{a1}}\right)+D\left(u_a-u_{C_{a2}}\right)=0 \\ (1-D)\left(u_a+u_{C_{a2}}-u'_a\right)+D\left(u_a+u_{C_{a2}}\right)=0 \end{cases} \tag{4}$$

The following can be obtained by Eq. (4):

$$u'_a=\frac{1}{1-2D}u_a \tag{5}$$

The boost factor B is:

$$B=\frac{1}{1-2D} \tag{6}$$

It can be seen from Eq. (6) that the boosting factor B can be changed by changing the through-duty ratio D. Since $0 < D < 0.5$, the boosting factor $B > 1$. Thus, the voltage transfer ratio can be made bigger than 0.866.

IV. PMSM BASED ON A PCHD MODEL AND PBC CONTROL

A. Establishment of a PCHD Model of a PMSM

A port dissipative Hamiltonian model in the form of a system state equation [24] is given by Eq. (7).

$$\left.\begin{aligned} \dot{\boldsymbol{x}}=\boldsymbol{f}(\boldsymbol{x})+\boldsymbol{g}(\boldsymbol{x})\boldsymbol{u}=[\boldsymbol{J}(\boldsymbol{x})\text{-}\boldsymbol{R}(\boldsymbol{x})]\frac{\partial H(\boldsymbol{x})}{\partial \boldsymbol{x}}+\boldsymbol{g}(\boldsymbol{x})\boldsymbol{u} \\ \boldsymbol{y}=\boldsymbol{h}(x)=\boldsymbol{g}^{\mathrm{T}}(\boldsymbol{x})\frac{\partial H(\boldsymbol{x})}{\partial \boldsymbol{x}} \end{aligned}\right\} \tag{7}$$

Where $\boldsymbol{x}$ is the state variable, $\boldsymbol{x}\in\mathbf{R}^n$; $\boldsymbol{u}$ and $\boldsymbol{y}$ are the input and output variables, $\boldsymbol{u}$ and $\boldsymbol{y}\in\mathbf{R}^m$; $\boldsymbol{R}(\boldsymbol{x})$ is the system port damping matrix, which satisfies $\boldsymbol{R}(\boldsymbol{x})=-\boldsymbol{R}^{\mathrm{T}}(\boldsymbol{x})\geq 0$; $\boldsymbol{J}(\boldsymbol{x})$ is the internal interconnect matrix of the system, which satisfies $\boldsymbol{J}(\boldsymbol{x})=-\boldsymbol{J}^{\mathrm{T}}(\boldsymbol{x})$; $\boldsymbol{H}(\boldsymbol{x})$ is the system energy storage function; and $\boldsymbol{f}(\boldsymbol{x})$ is the state variable function. $\boldsymbol{g}(\boldsymbol{x})$ is the input variable coefficient function.

The mathematical model of a PMSM in the dq coordinate system obtained by a PARK transformation is:

$$\begin{cases} L_d\dfrac{\mathrm{d}}{\mathrm{d}t}i_d=-Ri_d+n_p\omega L_q i_q+u_d \\ L_q\dfrac{\mathrm{d}}{\mathrm{d}t}i_q=-Ri_q-n_p\omega(L_q i_q+\varphi_f)+u_q \\ J\dfrac{\mathrm{d}\omega}{\mathrm{d}t}=n_p[(\mathrm{L_d}-\mathrm{L_q})i_d i_q+\varphi_f i_q]-T_L \end{cases} \tag{8}$$

where u_d and u_q are the stator voltage d-q axis components, and i_d and i_q are the stator current d-q axis components. R is the stator resistance. n_p is the number of rotor pole pairs. L_d and L_q are the stator inductances in the dq coordinate system. ω is the rotor mechanical speed. φ_f is the flux linkage of the permanent magnet. T_L is the load torque.

Define the state variable $\boldsymbol{x}$, input variable $\boldsymbol{u}$, and output variable $\boldsymbol{y}$ of the PMSM as:

$$\boldsymbol{x} = \begin{bmatrix} x_1 \\ x_2 \\ x_3 \end{bmatrix} = \begin{bmatrix} L_d i_d \\ L_q i_q \\ J\omega \end{bmatrix} = \boldsymbol{D} \begin{bmatrix} i_d \\ i_q \\ \omega \end{bmatrix} \tag{9}$$

$$\boldsymbol{u} = \begin{bmatrix} u_d & u_q & -T_L \end{bmatrix}^T, \quad \boldsymbol{y} = \begin{bmatrix} i_d & i_q & \omega \end{bmatrix}^T \tag{10}$$

$\boldsymbol{D}$ is a diagonal matrix, $\boldsymbol{D} = \text{diag}\ \{L_d, L_q, J\}$.

The energy storage function of the PMSM system can be expressed as:

$$H(\boldsymbol{x}) = \frac{1}{2}\boldsymbol{x}^T\boldsymbol{D}^{-1}\boldsymbol{x} = \frac{1}{2}\left[\frac{1}{L_d}x_1^2 + \frac{1}{L_q}x_2{}^2 + \frac{1}{J}x_3^2\right] \tag{11}$$

The dq mathematical model of PMSM can be expressed in the form of (7) PCHD:

$$\begin{bmatrix} \dot{x}_1 \\ \dot{x}_2 \\ \dot{x}_3 \end{bmatrix} = \left[\boldsymbol{J}(x) - \boldsymbol{R}(x)\right] \begin{bmatrix} i_d \\ i_q \\ \omega \end{bmatrix} + \boldsymbol{g}(\boldsymbol{x}) \begin{bmatrix} u_d \\ u_q \\ -T_L \end{bmatrix} \tag{12}$$

$$\boldsymbol{y} = \boldsymbol{g}^T(\boldsymbol{x})\frac{\partial \boldsymbol{H}(\boldsymbol{x})}{\partial \boldsymbol{x}} = \begin{bmatrix} i_d & i_q & \omega \end{bmatrix}^T \tag{13}$$

where:

$$\boldsymbol{J}(\boldsymbol{x}) = \begin{bmatrix} 0 & 0 & n_p x_2 \\ 0 & 0 & -n_p(x_1 + \varphi_f) \\ -n_p x_2 & n_p(x_1 + \varphi_f) & 0 \end{bmatrix}$$

$$\boldsymbol{R}(\boldsymbol{x}) = \begin{bmatrix} R & 0 & 0 \\ 0 & R & 0 \\ 0 & 0 & 0 \end{bmatrix}, \quad \boldsymbol{g}(\boldsymbol{x}) = \begin{bmatrix} 1 & 0 & 0 \\ 0 & 1 & 0 \\ 0 & 0 & 1 \end{bmatrix}$$

B. IDA-PBC Principle based on the PCHD Model

In order to stabilize the PMSM system at the equilibrium point $\boldsymbol{x}^*$, a closed-loop expected energy function $H_d(\boldsymbol{x})$ is constructed by feedback control so that $H_d(\boldsymbol{x})$ it at its minimum at $\boldsymbol{x}^*$. At the same time, the feedback control law $\boldsymbol{u}=\boldsymbol{\beta}(\boldsymbol{x})$ is designed. Thus, the closed-loop system can be expressed as:

$$\dot{x} = \left[\boldsymbol{J}_d(\boldsymbol{x}) - \boldsymbol{R}_d(\boldsymbol{x})\right]\frac{\partial H_d}{\partial \boldsymbol{x}}(\boldsymbol{x}) \tag{14}$$

$\boldsymbol{J}_d(\boldsymbol{x})$ and $\boldsymbol{R}_d(\boldsymbol{x})$ are the desired interconnect matrix and damping matrix, respectively. They satisfy:

$$\begin{cases} \boldsymbol{J}_d(\boldsymbol{x}) = \boldsymbol{J}(\boldsymbol{x}) + \boldsymbol{J}_a(\boldsymbol{x}) = -\boldsymbol{J}_d^T(\boldsymbol{x}) \\ \boldsymbol{R}_d(\boldsymbol{x}) = \boldsymbol{R}(\boldsymbol{x}) + \boldsymbol{R}_a(\boldsymbol{x}) = \boldsymbol{R}_d^T(\boldsymbol{x}) \geq 0 \end{cases}$$

If the designed feedback law $\boldsymbol{u}=\boldsymbol{\beta}(\boldsymbol{x})$, $\boldsymbol{R}_a(\boldsymbol{x})$, $\boldsymbol{J}_a(\boldsymbol{x})$ and $\boldsymbol{K}(\boldsymbol{x})$ can satisfy [24]:

$$\left[\boldsymbol{J}_d(\boldsymbol{x}) - \boldsymbol{R}_d(\boldsymbol{x})\right]\boldsymbol{K}(\boldsymbol{x}) = -\left[\boldsymbol{J}_a(\boldsymbol{x}) - \boldsymbol{R}_a(\boldsymbol{x})\right]\frac{\partial H(\boldsymbol{x})}{\partial \boldsymbol{x}} + \boldsymbol{g}(\boldsymbol{x})\boldsymbol{\beta}(\boldsymbol{x}) \tag{15}$$

the following is obtained:

$$\begin{cases} \dfrac{\partial \boldsymbol{K}(\boldsymbol{x})}{\partial \boldsymbol{x}} = \left[\dfrac{\partial \boldsymbol{K}(\boldsymbol{x})}{\partial \boldsymbol{x}}\right]^T, \dfrac{\partial \boldsymbol{H}_d(\boldsymbol{x}^*)}{\partial \boldsymbol{x}} = 0, \dfrac{\partial^2 \boldsymbol{H}_d(\boldsymbol{x}^*)}{\partial \boldsymbol{x}^2} > 0 \\ H_d(\boldsymbol{x}) - H(\boldsymbol{x}) = H_a(\boldsymbol{x}), \dfrac{\partial H_a(\boldsymbol{x})}{\partial \boldsymbol{x}} = \boldsymbol{K}(\boldsymbol{x}) \end{cases} \tag{16}$$

The closed loop system is a PCHD system, and $\boldsymbol{x}^*$ is a stable balance point of the system. $H_a(\boldsymbol{x})$ is the energy function to be determined by the feedback system.

V. STABILITY ANALYSIS AND CONTROLLER DESIGN

A. Stability Analysis

The goal of the PMSM drive system is to achieve the tracking of a desired speed ω^*. In order to satisfy the maximum torque control, the basic idea of the vector control is to use i_d=0 control. If the load is known at this time, the desired balance point is [24]:

$$\boldsymbol{x}^* = \begin{bmatrix} x_1^* & x_2^* & x_3^* \end{bmatrix}^T = \begin{bmatrix} 0 & \dfrac{L_q T_L}{n_p \varphi_f} & J\omega^* \end{bmatrix}^T \tag{17}$$

Take the expected Hamiltonian function as [24]:

$$H_d(\boldsymbol{x}) = \frac{1}{2}(\boldsymbol{x} - \boldsymbol{x}^*)^T \boldsymbol{D}^{-1}(\boldsymbol{x} - \boldsymbol{x}^*) \tag{18}$$

From Eq. (16), the following can be obtained:

$$\begin{cases} \dfrac{\partial H_d(\boldsymbol{x})}{\partial \boldsymbol{x}} = \boldsymbol{D}^{-1}(\boldsymbol{x} - \boldsymbol{x}^*), \dfrac{\partial H_d(\boldsymbol{x})}{\partial \boldsymbol{x}^2} = \boldsymbol{D}^{-1}, \dfrac{\partial H(\boldsymbol{x})}{\partial \boldsymbol{x}} = \boldsymbol{D}^{-1}\boldsymbol{x} \\ \boldsymbol{K}(\boldsymbol{x}) = \dfrac{\partial H_a(\boldsymbol{x})}{\partial \boldsymbol{x}} = \dfrac{\partial H_d(\boldsymbol{x})}{\partial \boldsymbol{x}} - \dfrac{\partial H(\boldsymbol{x})}{\partial \boldsymbol{x}} = -\boldsymbol{D}^{-1}\boldsymbol{x}^* \end{cases} \tag{19}$$

When $\boldsymbol{x} = \boldsymbol{x}^*$, $\dfrac{\partial H_d(\boldsymbol{x})}{\partial \boldsymbol{x}} = 0$ and $\dfrac{\partial^2 H_d(\boldsymbol{x})}{\partial \boldsymbol{x}^2} > 0$, Eq. (16) can be verified by Eq. (19). Therefore, the passivity-based control system in this paper is progressively stable near the equilibrium point.

B. Controller Design

It can be assumed that:

$$\boldsymbol{J}_a(\boldsymbol{x}) = \begin{bmatrix} 0 & -J_{12} & J_{13} \\ J_{12} & 0 & J_{23} \\ -J_{13} & -J_{23} & 0 \end{bmatrix}, \quad \boldsymbol{R}_a(\boldsymbol{x}) = \begin{bmatrix} r_1 & 0 & 0 \\ 0 & r_2 & 0 \\ 0 & 0 & 0 \end{bmatrix} \tag{20}$$

where: J_{12}, J_{13} and J_{23}, and r_1 and r_2 are the interconnection and damping parameters to be determined respectively [24]. By substituting equation (20) into equation (15), the following can be obtained:

$$\left[\boldsymbol{J}_d(\boldsymbol{x}) - \boldsymbol{R}_d(\boldsymbol{x})\right]\boldsymbol{D}^{-1}\boldsymbol{x}^* = \left[\boldsymbol{J}_a(\boldsymbol{x}) - \boldsymbol{R}_a(\boldsymbol{x})\right]\boldsymbol{D}^{-1}x - \boldsymbol{g}(\boldsymbol{x})\boldsymbol{\beta}(\boldsymbol{x}) \tag{21}$$

By substituting $\boldsymbol{J}_d(\boldsymbol{x})$, $\boldsymbol{R}_d(\boldsymbol{x})$, $\boldsymbol{J}_a(\boldsymbol{x})$, $\boldsymbol{R}_a(\boldsymbol{x})$, $\boldsymbol{g}(\boldsymbol{x})\boldsymbol{\beta}(\boldsymbol{x})$ and $\boldsymbol{x}^*$ into equation (21), the following can be obtained:

$$J_{23}(x_2 - x_2^*) = n_p x_1(x_2^* + \frac{J_{13}L_q}{L_d n_p}) \tag{22}$$

To ensure that Eq. (22) is always established, take

TABLE I
PARAMETERS OF THE PMSM AND QUASI-Z SOURCE

Parameters	Values	Parameters	Values
V_r	311 V	J	0.0008 kg· m^2
f_i	50 Hz	R	0.958 Ω
φ_f	0.183 Wb	L_s	5.25 mH
i_r	6.5 A	n_p	4
ω_r	1600 r/min	L_z	0.05 mH
T_r	14.8 N·m	C_z	50 μF

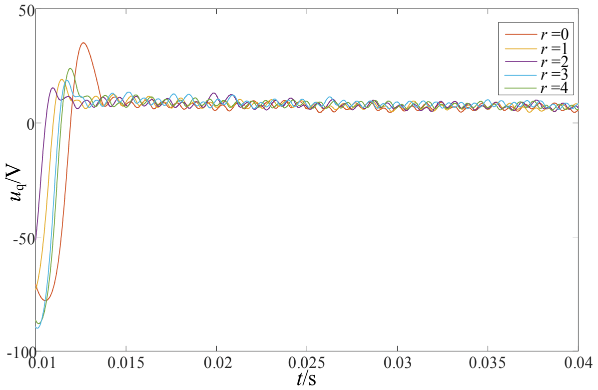

Fig. 4. Waveforms of u_q with different values of r.

$J_{23} = -n_p x_1$, $J_{13} = -L_d / L_q n_p x_2$ and $J_{12} = -kx_3$. k is a free parameter whose value does not affect system stability.

Substituting J_{23}, J_{13} and J_{12} into Eq. (21), it becomes possible to derive the dq axis output voltage. The control law of passivity-based control is:

$$\begin{cases} u_d = -r_1 i_d + \left(kJ - n_p L_q\right) i_q \omega - \dfrac{kJT_L}{n_p \varphi_f}\omega \\ u_q = -r_2 i_q + \left(n_p L_d - kJ\right) i_d \omega + n_p \varphi_f \omega^* + \left(R_s + r_2\right) \dfrac{T_L}{n_p \varphi_f} \end{cases} \tag{23}$$

VI. SIMULATIONS

In order to verify the feasibility and superiority of a quasi-Z source matrix converter (QZMC) applied in a PMSM passivity-based control (PBC) drive system, the system is simulated in MATLAB/Simulink software. The parameters of the PMSM and quasi-Z source are shown in Table I.

In Table I, V_r, i_r, ω_r and T_r are the rated voltage, current, rotating speed and torque of the PMSM, respectively. L_z and C_z are the inductance and capacitance values of the Z source network.

In order to study the influence of injection damping $r(r_1=r_2=r)$ on the control effect, this paper changes the magnitude of r and observes the output q-axis voltage u_q, which can be obtained as shown in the Fig. 4.

It can be seen from Fig. 4 that when r is increased from 0 to 2, the overshoot and the time to reach stability gradually decrease. After exceeding 2, these values increase again. The curve in Fig. 4 indicates that the injection damping size affects the overshoot and stability time. When r is around 2, the response curve is almost ideal. Thus, this paper uses r=2. The parameter k(k=100) is a free parameter that does not affect the stability of the system. Therefore, in this paper $r=r_1=r_2=2$, k=100.

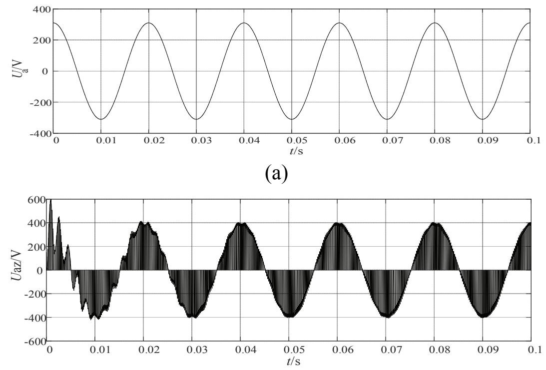

(a)

(b)

Fig. 5. Simulation results of a quasi-Z source voltage boost. (a) A-phase output voltage of an AC power supply. (b) A-phase output voltage of a quasi-Z source network QZMC-PMSM.

A. Voltage Boost Situation

In order to verify whether the boosting capability of the quasi-Z source network satisfies the formula B=1/(1-2D), the phase voltage of the three-phase AC power supply is set to 311V, and the through-duty D is set to 0.1. Theoretically, the boost factor B is 1.25, and Z-source output phase voltage should be 388.75V.

Fig. 5 shows simulation results of the boosting capability of a quasi-Z source. The phase voltage obtained by the three-phase power supply and the output phase voltage obtained by the quasi-Z source boosting are shown in Fig. 5(a) and Fig. 5(b). It can be seen from these figures that the a-phase output voltage of the quasi-Z source network is indeed 388V, which satisfies the boosting formula.

Fig. 6(a) and Fig. 6(b) show the DC bus voltage of the TSMC and QZMC, respectively. Fig. 6(c) and Fig. 6(d) show the line voltages of the TSMC and QZMC outputs, respectively. It can be seen from Fig. 6(a), 6(b), 6(c) and 6(d) that when the quasi-Z source is added to the TSMC, the DC bus voltage and the output line voltage are both increased, and the QZMC voltage transmission ratio is about 1. With a voltage transfer ratio of 1, it can be ensured that the PMSM operates at the rated voltage when it is driven, which is important for good operation of the PMSM.

B. PMSM Control Result of PID and PBC

1) Constant Speed: Set the phase voltage of the three-phase input to 220V, and boost the PMSM stator voltage to 220V through the quasi-Z network boost. Simulate the QZMC-PMSM system speed when the load is known. The simulation results are shown in Fig. 7(a). The speed is 1000r/min and the load is 5N·m. It can be seen from this figure that the PMSM

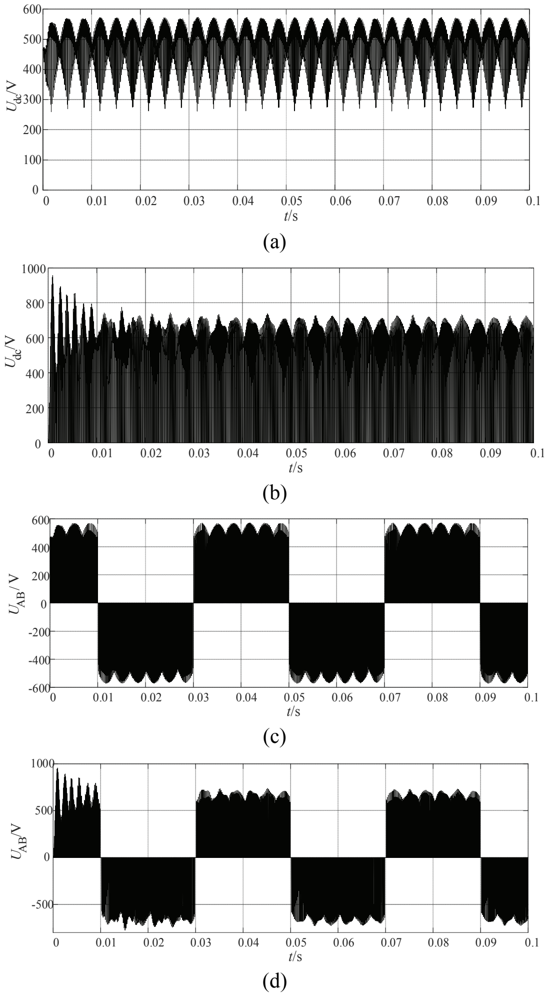

Fig. 6. Simulation result of an MC voltage boost. (a) DC bus voltage of the TSMC. (b) DC bus voltage of the QZMC. (c) Output line voltage of the TSMC. (d) Output line voltage of the QZMC.

can reach and stabilize at a given speed under the two control methods of PBC and PID in the inverter stage. When compared with the PID control, the PBC control of this paper can make the overshoot 0, and the dynamic response speed is improved.

2) Given Speed Changes: In order to verify the speed regulation capability of the QZMC-PMSM system, the load is kept constant at 5 N·m. When the motor is operated at 0~0.2 s, the rated motor speed is 1600 r/min, and the speed is reduced to 1000 r/min at 0.2 s. Simulation results are shown in Fig. 7(b). It can be seen from this figure that the system under the control of the PBC can track a given speed without overshoot. It can also be seen that the system can adjust the speed faster and that the dynamic performance of the system is better when the speed is changed.

3) Load Changes: The system was simulated under a load disturbance and the PMSM speed was set to 600 r/min. From 0 to 0.2 s, the load is 5 N·m, and at 0.2 s, the load abruptly changes to 10 N·m. The speed simulation is shown in Fig. 7(c).

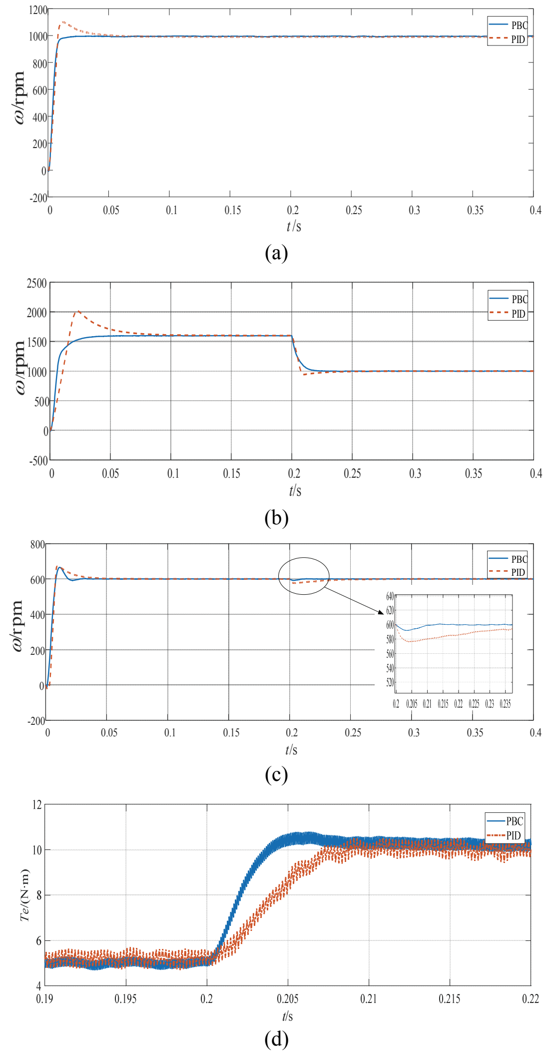

Fig. 7. Comparison of PID and PBC simulation results. (a) Speed curve when the speed is constant. (b) Speed curve when the speed changes. (c) Speed curve comparison when the load changes. (d) Torque curve comparison when the load changes.

As can be seen from this figure, the PBC control speed curve is over-adjusted. However, it can be quickly stabilized at a given speed. When the load changes at 0.2 s, the PBC control can return to a given speed faster than the PID control method. In addition, the system is more robust.

Fig. 7(d) shows an electromagnetic torque curve under the two control methods of the PID and PBC when the load changes. As can be seen from the Fig. 7(d), the electromagnetic torque response of the PBC is better than that of the PID when the load changes.

VII. EXPERIMENT

In order to further verify the performance of the designed PMSM drive system, an experiment was carried out on the experimental platform shown in Fig. 8. The experimental parameters are consistent with the simulation parameters. The

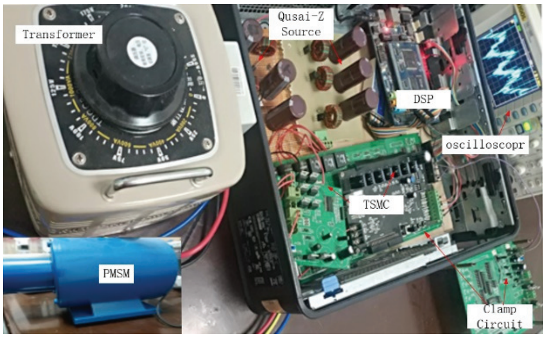

Fig. 8. Photo of experimental platform.

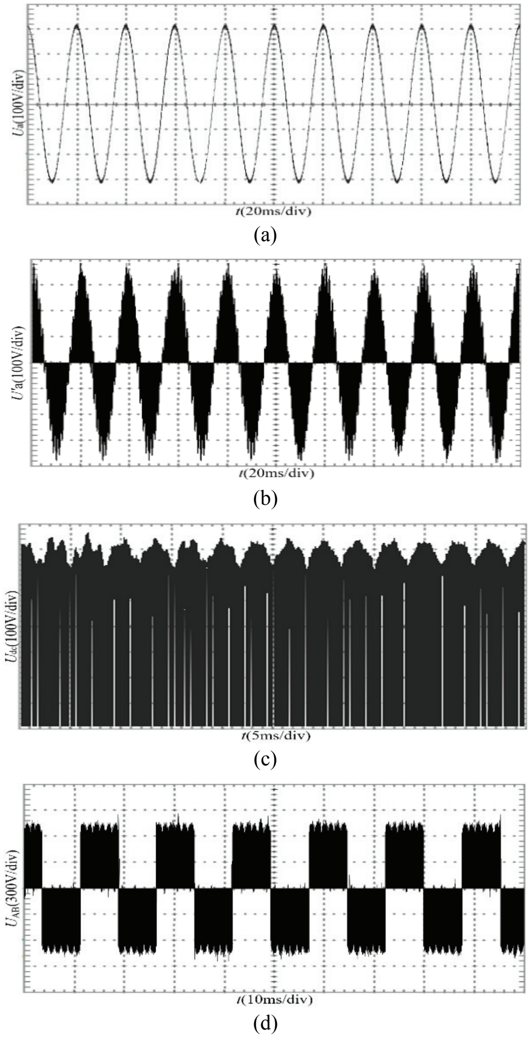

(a)

(b)

(c)

(d)

Fig. 9. Boost capacity experiments of the QZMC. (a) A-phase input voltage from the gird. (b) Quasi-Z source a-phase output voltage. (c) DC bus voltage. (d) Output line voltage of the QZMC.

control was carried out using a XC3S1800A digital signal processor (DSP). The bidirectional switch of the QZMC is a SK60GM123, and it is driven by a drive module 6SD106EI.

A. Boost Capacity and Constant Speed Control

In the matrix converter experiment, the input AC voltage is a 220V/50Hz grid voltage. Fig. 9(a) is an a-phase input voltage waveform. Fig. 9(b) is the quasi-Z source a-phase output voltage. Fig. 9(c) is the DC bus voltage. Fig. 9(d) is the output line voltage U_{AB}. By analyzing these experimental results, the same conclusion reached in part *A* in Section VI are obtained. After adding the quasi-Z source to the TSMC, the DC bus voltage and the output line voltage are both increased, and the QZMC voltage transmission ratio can reach 1. Figs.10-12 show speed curves of the PMSM using the PBC and PID methods. The hardware experiment results show that the speed overshoot is small and the dynamic response speed is improved under the control of the PBC.

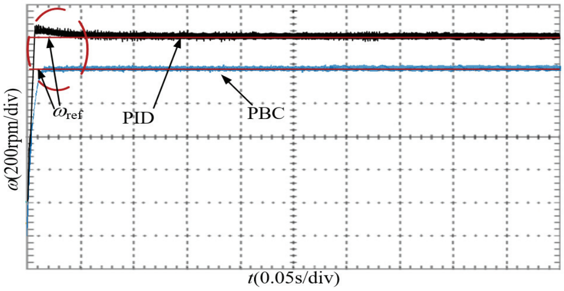

Fig. 10. Speed comparison when run at a constant speed.

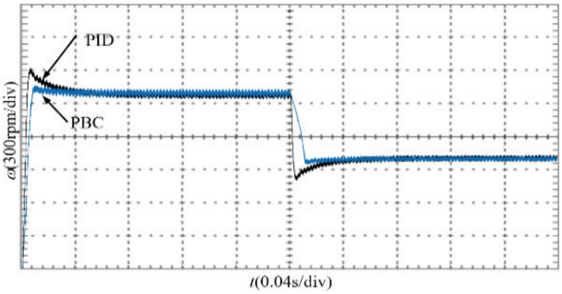

Fig. 11. Speed comparison when the speed changes.

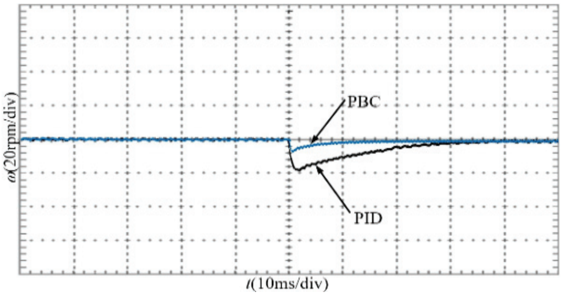

Fig. 12. Speed comparison when the load changes.

B. Variable Speed Control and Load Disturbance

Fig. 10 shows a comparison of experiment result when the PMSM runs at a constant speed under the PBC and PID methods. When the speed and load of the PMSM change, experimental waveforms of the QZMC-PMSM passivity-based control system designed in this paper and the traditional PID control are shown in Fig. 11 and Fig. 12, respectively. It can be seen from these waveform that the system with the PBC control has a stronger anti-interference capability and improved dynamic performance.

VIII. CONCLUSION

In this paper, a passivity-based control (PBC) system for quasi-Z source matrix converter (QZMC)-permanent magnet synchronous motors (PMSMs) is designed. A current-continuous quasi-Z-source two-stage matrix converter with boosting capability is used to replace the traditional PWM converter. A PCHD-based nonlinear passivity-based controller is designed for PMSMs, and the stability of the control system is theoretically verified. Finally, simulations and experiments were carried out on MATLAB and an experimental platform. Through the analysis and experiment in this paper, the following conclusions are obtained.

1) The through-vector is inserted into the rectifier stage through the quasi-Z source. Thus, the output voltage of the quasi-Z source is greater than the input voltage, which ensures that the voltage transmission ratio of the QZMC can reach or even exceed 1. This in turn, improves the speed regulation range and working performance of the driven PMSM.

2) When compared with the traditional PID control, the passivity-based control QZMC-PMSM drive system proposed in this paper has better dynamic and static performance and stronger anti-interference capability.

ACKNOWLEDGMENT

This work has been supported by National Natural Science Foundation of China (61573239) and Shanghai Key Laboratory Power Station Automation Technology Laboratory (13DZ22 73800).

REFERENCES

[1] S. Morimoto, Y. Asano, and T. Kosaka, "Recent technical trends in PMSM," in *2014 International Power Electronics Conference,* pp. 1997-2003, 2014.

[2] O. Aydogmusb and E. Deniz, "Design and implementation of two-phase permanent magnet synchronous motor fed by a matrix converter," *IET Power Electron*., Vol. 10, No. 9, pp. 1054-1060, Jul. 2017.

[3] P. Szczesniak and J. Kaniewski, "Power electronics converters without DC energy storage in the future electrical power network," *Electr. Power Syst. Res.*, Vol. 129, pp. 194-207, Dec. 2015.

[4] E. E. M. Mohamed and M. A. Sayed, "Matrix converters and three-phase inverters fed linear induction motor drives-Performance compare," *Ain Shams Eng. J.*, Vol. 9, No. 3, pp. 329-340, Sep. 2018.

[5] R. T. Ugale and B. N. Chaudhari, "Rotor configurations for improved starting and synchronous performance of line start permanent-magnet synchronous motor," *IEEE Trans Ind. Electron*., Vol. 64, No. 1, pp. 138-148, Jan. 2017.

[6] G. T. Chiang and J.-i. Itoh, "Comparison of two overmodulation strategies in an indirect matrix converter," *IEEE Trans Ind Electron*., Vol. 60, No. 1, pp43-53, Jan. 2013.

[7] S. Liu, B. M. Ge, and Y. S. Liu, "Modeling, analysis, and parameters design of LC-filter-integrated quasi-Z-source indirect matrix converter," *IEEE Trans Power Electron*., Vol. 31, No. 11, pp. 7544-7555, Nov. 2016.

[8] M. Alizadeh and S. S. Kojuri, "Modelling, control, and stability analysis of quasi-Z-source matrix converter as the grid interface of a PMSG-WECS," *IET Gener. Transm. Distribut.*, Vol. 11, No. 14, pp. 3576-3585, Sep0. 2017.

[9] O. Ellabban, H. Abu-Rub, and B. M. Ge, "A quasi-Z-source direct matrix converter feeding a vector controlled induction motor drive," *IEEE J. Emerg. Sel. Top Power Electron.*, Vol. 3, No. 2, pp. 339-348, Jun. 2015.

[10] D. S. Vidhya and T. Venkatesan, "Quasi-Z-source indirect matrix converter fed induction motor drive for flow control of dye in paper mill," *IEEE Trans Power Electron.*, Vol. 33, No. 2, pp.1476-1486, Feb. 2018.

[11] S. M. Tripathi, A. N. Tiwari, and D. Singh, "Grid-integrated permanent magnet synchronous generator based wind energy conversion systems: A technology review," *Renew. Sustain. Energy Rev.*, Vol. 51, pp. 128-1305, Nov. 2015.

[12] N. Anh Tuan, M. S. Rafaq, H. H. Choi, and J.-W. Jung, "A model reference adaptive control based speed controller for a surface-mounted permanent magnet synchronous motor drive," *IEEE Trans Ind Electron.*, Vol. 65, No. 12, pp. 9399-9409, Dec. 2018.

[13] A. Hosseyni, R. Trabelsi, and M.F. Mimouni, "Sensorless sliding mode observer for a five-phase permanent magnet synchronous motor drive," *ISA Trans.*, Vol. 58, pp. 462-473, Sep. 2015.

[14] L. Xiong, P. Li, H. Li, and J. Wang, "Sliding mode control of DFIG wind turbines with a fast exponential reaching law," *Energies.*, Vol. 10, No. 11, Nov. 2017.

[15] J. Linares-Flores, C. Garcia-Rodriguez, and H. Sira-Ramirez, "Robust backstepping tracking controller for low-speed PMSM positioning system: design, analysis, and implementation," *IEEE Trans Ind Informat.*, Vol. 11, No. 5, pp. 1130-1141, Oct. 2015.

[16] C. H. Lin, "Nonlinear backstepping control design of lsm drive system using adaptive modified recurrent laguerre orthogonal polynomial neural network," *Int. J. Contr. Autom. Syst.*, Vol. 15, No. 2, pp. 905-917, Apr. 2017.

[17] F. J. Lin, S. G. Chen, and I. F. Sun, "Adaptive backstepping control of six-phase PMSM using functional link radial basis function network uncertainty observer," *Asian J. Contr.*, Vol. 19, No. 6, pp. 2255-2269, Nov. 2017.

[18] B. Belabbes and A. Larbaoui, "Passive control by backstepping of the synchronous motor," *Rev. Roum. Sci. Tech-El*, Vol. 60, No. 3, pp. 333-342, Jul./Sep. 2015.

[19] H. Komurcugil, "Improved passivity-based control method and its robustness analysis for single-phase uninterruptible power supply inverters," *IET Power Electron*., Vol. 8, No. 8, pp. 1558-1570, Aug. 2015.

[20] L. Harnefors, A.G. Yepes, and A. Vidal, "Passivity-based controller design of grid-connected VSCs for prevention of electrical resonance instability," *IEEE Trans Ind Electron.*, Vol. 62, No. 2, pp. 702-710, Feb. 2015.

[21] J. Huang, H. Wang, and C. Wang, "Passivity-based control of a doubly fed induction generator system under unbalanced grid voltage conditions," *Energies.*, Vol. 10, No. 8, Aug. 2017.

[22] M. Z. Guo, Y. S. Liu, and B. M. Ge, "Optimum boost control of quasi-z source indirect matrix converter," *IEEE Trans Ind Electron.*, Vol. 65, No. 10, pp. 8393-8404, Oct.

2018.

[23] M. Khanchoul, M. Hilairet, and D. Normand-Cyrot, "A passivity-based controller under low sampling for speed control of PMSM," *Contr. Eng. Practice*., Vol. 26, No. 1, pp. 20-27, May 2014.

[24] X. Fan, L. Guan, C. Xia, and T. Ji, "IDA-PB control design for VSC-HVDC transmission based on PCHD model," *Int. Trans. Electr. Energy Syst.*, Vol. 25, No. 10, pp. 2133-2143, Oct. 2015.

Qiming Cheng was born in Yancheng, Jiangsu, China. He received his B.S. degree in Physics from Suzhou University, Suzhou, China, in 1984; and his M.S. degree in Electrical Engineering from Zhejiang University, Hangzhou, China, in 1988. In 2001, he joined the Shanghai University of Electric Power, Shanghai, China. He has presided over several key scientific research projects such as a Shanghai Key Science and Technology Research Project and a Shanghai Municipal Education Commission Key Natural Fund. He is presently working as a Professor and as a Master Tutor in the College of Automation Engineering, Shanghai University of Electric Power. His current research interests include power electronics and control, which include ac machine drives, new energy generation, microgrid control, and electric vehicle and charging station control.

Lin Wei was born in China, in 1995. He received his B.S. degree in Measurement and Control Technology and Equipment from North Eastern University, Shenyang, China, in 2017. He is presently working towards his M.S. degree at the Shanghai University of Electric Power, Shanghai, China. His current research interests include electric power systems automation and advanced motor control in various industrial fields.